2000년 춘계물리학회

28 – 29 April, 2000

육군사관학교

Impurity effects on ECH preionization for KSTAR*

배 영순, 조 무현, Owen C. Eldridge, 남궁 원
포항공과대학교
and Alan C. England
기초과학지원연구소

* *Work supported by KAERI and KBSI*

Abstract

We investigated ECH preionization for KSTAR including impurities such as carbon and oxygen with the ECH preionization code. The electron energy can be lost through the impurity radiation. We also calculated the ion energy density which can be lost by the charge exchanges between hydrogen ions and hydrogen atoms. In this paper, we present the simulation results; the final electron temperature and density are decreased by the impurity ions.

Introduction

Preionization has been successfully applied in a variety of tokamaks and is normally used to produce the plasma in contemporary stellarators. The general conclusion of these experiments was that ECH was effective in producing a good plasma which would (a) reduce the startup runaway electrons, (b) reduce the voltage required to start the plasma current and (c) somewhat reduce the Volt-sec expenditure from the transformer needed to establish the plasma. The motivation for many of those experiments was the pioneering work of Pent et al. [1]. While some of the predictions of the theory were not borne out by the experiments, nevertheless, the theory was important in showing the value of preionization for voltage reduction. On the basis of the experimental work by Kulchar et al. [2], a model was produced which was able to adequately describe the experiments in ISX-B. Later experimental work included the large tokamak experiments in T-10 [3] and DIII-D [4]. The Modeling efforts of Fidone and Granata [5] showed that for a large tokamak, energy deposition would not occur at the Electron Cyclotron Resonance Heating (ECRH) layer. Maroli and Petrillo [6] added plasma radial growth and impurities. Lloyd et al. [7] produced a more advanced model and added the effect of impurities, but neglected the error field effects. The work of Lloyd et al. was used at KBSI to produce a code called TSTART [8] that included error field effects.

The code and the equations have been described in detail in this paper.

The input parameters correspond to KSTAR are as follows:

(1) a major radius $\boldsymbol{R}$ of 180 cm,

(2) a minor radius $\boldsymbol{a}$ of 50 cm,

(3) an error field range $\boldsymbol{B_{err}}$ from 0 to 5 mT,

(4) a primary voltage $\boldsymbol{V_{pri}}$ of up to 200 V,

(5) an RF power $\boldsymbol{P_{rf}}$ at 84 GHz up to 500 kW,

(6) an initial neutral density $\boldsymbol{n_0}$ from 0.2 x 10^{13} cm^{-3} to 1.0 x 10^{13} cm^{-3},

(7) an RF pulse duration $\boldsymbol{T_{rf}}$ up to 1 s, and

(8) a magnetic field B of 3 T,

(9) a carbon impurity fraction, ***fci*** from 0 to 0.02,

(10) an oxygen impurity fraction, ***foi*** is always set to 2 times *fci*.

The quantities in boldface can be used as variables. For all of the calculations that are described here, the preionization was always started 10 ms before the loop voltage was applied. In this present set of calculations, the effect of variation of the initial minor radius $\boldsymbol{a}$ is not examined. The present code version is the fortran version transferred from the basic version made by Dr. Owen C. Eldridge. The fortran version has the impurity power radiation calculation. Previously it has also been found that the best results are obtained with a parallel index of refraction, $n_{||}$ of 0.5 and 100 % x-mode polarization.

The preionization model

The equations written in the code are summarized and their references are described.

1. The continuity equation

$$\frac{dn_e}{dt} = n_e \nu_{ion} - n_e (\nu_{err} + \nu_{dr} + \nu_{diff}) \qquad (1)$$

where, ν_{ion} is the ionization rate, ν_{err} is the loss rate due to error field, ν_{dr} is the loss rate due to the toroidal drift, and ν_{diff} is the loss rate due to the diffusion.

2. Particle balance

$$\frac{dn_0}{dt} = -\frac{dn_e}{dt} \qquad (2)$$

where, n_0 is the neutral density.

3. Energy balance

$$\frac{dU_e}{dt} = \frac{P_{ECH} + P_{OH} - P_{RAD}}{V} - U_e(\nu_{err} + \nu_{dr} + \nu_E) - \frac{1}{V}(P_{EQU} + P_{BREM} + P_{IRAD})$$

$$\frac{dU_i}{dt} = \frac{1}{V}(P_{EQU} - P_{CX}) - U_i \nu_E \qquad (3)$$

where,

$\boldsymbol{U}_{\mathbf{e}}$: electron energy density, $\boldsymbol{U}_{\mathbf{i}}$: ion energy density,

$\boldsymbol{P}_{\mathbf{ECH}}$: ECH power, $\boldsymbol{P}_{\mathbf{OH}}$: Ohmic heating power,

$\boldsymbol{P}_{\mathbf{RAD}}$: The radiation power loss (entirely due to ionization process),

$\boldsymbol{P}_{\mathbf{EQU}}$: Electron-ion equipartition power loss,

$\boldsymbol{P}_{\mathbf{BREM}}$: The bremsstrahlung power loss (hydrogen ions & impurity ions),

$\boldsymbol{P}_{\mathbf{CX}}$: The charge exchange power loss (hydrogen atom and hydrogen ions),

$\boldsymbol{P}_{\mathbf{IRAD}}$: The impurity radiaion power loss (Carbon and Oxygen, etc.),

and, the ν_{E} is the energy confinement time.

4. Equivalent circuit equation

$$V_0 - I_{pri}R_{pri} - L_{pri}\frac{dI_{pri}}{dt} - M\frac{dI_p}{dt} = 0$$

$$I_pR_p + L_p\frac{dI_p}{dt} + M\frac{dI_{pri}}{dt} = 0$$

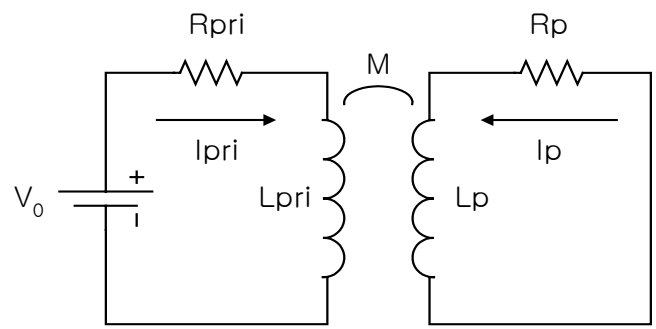

→

$$M_c^2\frac{dI_p}{dt} = -I_pR_pL_{pri} + I_{pri}R_{pri}M - V_0M$$

$$M_c^2\frac{dI_{pri}}{dt} = I_pR_pM - I_{pri}R_{pri}L_p + V_0L_p \qquad \textbf{(4)}$$

where, $M = k\sqrt{L_{pri}.L_p}$ is the mutual inductance and $M_c^2 = L_{pri}L_p - M^2$ is the cross inductance.
Loop voltage and resistive voltage of plasma

$$V_{loop} = -M\frac{dI_{pri}}{dt} = I_p R_p + L_p\frac{dI_p}{dt}$$
$$V_{res} = -I_p R_p \qquad (5)$$

KSTAR poloidal coil parameters

$R_{pri} = 0.8 \times 10^{-3}\,\Omega$, $L_{pri} = 5.0 \times 10^{-3}$ H, $k = 0.9$

Plasma resistance and inductance

- Plasma resistance [9]

$$R_p = \frac{L}{A}\eta = \frac{L}{A}\frac{1}{\sigma_{\parallel}} = \frac{2\pi R}{\pi a^2}\frac{1}{2\sigma_{\perp}}, \text{ and } \sigma_{\perp} = \frac{\omega_p^2}{4\pi(\nu_{ei}+\nu_{eo})} = \frac{1}{9\times10^9}\frac{n_e[cm^{-3}]}{(\nu_{ei}+\nu_{eo})} \times (2.82\times10^{-13})(9\times10^{20})$$

where, L is the total torus length, A is the torus cross section, and $\sigma_{\parallel} = 2\sigma_{\perp}$ is the conductivity.

- Plasma inductance [7]

$$L_p = \mu_0 R\left(\ln\frac{8R}{a} + \frac{l_i}{2} - 2\right)$$

For KSTAR (Operation Mode No. 4, $l_i = 0.5$ (flat current profile)) $L_p = \mu_0 R\left(\ln\frac{8R}{a} - 1.75\right)$

But we have used the form of "***Maroli & Petrillo***" [6] (this form is used in original codes of England and Eldridge.),

$$L_p = \mu_0 R\left(\ln\frac{8R}{a} - 0.75\right)$$

Rate Calculations [s^{-1}]

1. ν_{ion} (e + H process) [10]

$$\nu_{ion} = n_0 \langle \sigma v \rangle_{ion}$$
$$= n_0 Exp\left[\sum_{i=1}^{7} C_i \left[\ln\left(\frac{3}{2} e T_e \right) \right]^i \right]$$

C_1 = -31.7385, C_2 = 11.43818, C_3 = -3.833998, C_4 = 0.7046692, C_5 = -7.431486 E-02,
C_6 = 4.153749 E-03, C_7 = -9.486967 E-05

2. ν_{err} (The electron moves along the field line with their thermal velocity. The error field can be produced by Toroidal Field coil structure error. This loss is overcome when the poloidal field induced by the plasma current is same as the error field, and the plasma current is called "the critical current". The critical current is easily obtained from the Ampere's law but 2 factor, "***twice Alcator scaling***".)

$$\nu_{err} \approx \frac{\delta B}{B} \frac{V_T}{a} \left[1 - \frac{I_p}{I_c} \right], \quad I_c = 2 \frac{2\pi a \delta B}{\mu_0} = 1.0 \times 10^7 a \delta B \quad (I_p \geq I_c, \ \nu_{err} = 0)$$

where, δB is the error field, $V_T = \sqrt{T_e/m_e}$ is the electron thermal velocity, a is the plasma minor radius, I_p is the plasma current, and I_c is the critical current.

3. ν_{dr} (due to the curvature and gradient of B) [11]

$$\left|\vec{V}_R + \vec{V}_{\nabla B}\right| = \left|\frac{m_e}{q}\left(V_{\parallel}^2 + \frac{1}{2}V_{\perp}^2\right)\frac{\vec{R}_c \times \vec{B}}{R_c^2 B^2}\right| = \frac{2T_e}{R\omega_{ce} m_e}$$

$$\nu_{dr} = \frac{\left|\vec{V}_R + \vec{V}_{\nabla B}\right|}{a}\left(1 - \frac{I_p}{I_c}\right) = \frac{2T_e}{aR\omega_{ce} m_e}\left(1 - \frac{I_p}{I_c}\right) \quad (I_p \geq I_c,\ \nu_{dr} = 0)$$

where, R is the Tokamak major radius, and the ω_{ce} is the electron cyclotron frequency.

4. ν_{diff} (Ambipolar diffusion for hot plasma approximation, $T_e = T_i$) [12]

$$D_{\perp} = \frac{T_e \nu_m}{m\omega_{ce}^2}\left(1 + \frac{T_i}{T_e}\right) \approx 2\frac{T_e \nu_m}{m\omega_{ce}^2}$$

$$\text{since, } V_{\perp} = -D_{\perp}\frac{\nabla n}{n} = -D_{\perp}\frac{2}{a},$$

$$\nu_{diff} = \frac{V_{\perp}}{a/2} = \frac{8T_e \nu_m}{m\omega_{ce}^2 a^2} = \frac{8T_e\left(\nu_{ei} + \nu_{eo}\right)}{m\omega_{ce}^2 a^2}$$

where, ν_m is the momentum transfer frequency and is the sum of ν_{ei} (electron-ion collision frequency) and ν_{eo} (electron-neutral collision frequency).

where, ν_m is the momentum transfer frequency and is the sum of ν_{ei} (electron-ion collision frequency) and ν_{eo} (electron-neutral collision frequency).

- ν_{ei} [9]

$$T_e \le 10\ eV,\ \ln\Lambda = 23 - \ln\left(\sqrt{\frac{n_e}{T_e^3}}\right)$$

$$T_e > 10\ eV,\ \ln\Lambda = 24 - \ln\left(\frac{\sqrt{n_e}}{T_e}\right)$$

$$\nu_{ei} = \frac{n_e \ln\Lambda}{3.44\times10^5 (T_e)^{3/2}}$$, where lnΛ is the Coulomb logarithm.

- ν_{eo} [9]

$$\nu_{eo} = n_0 \sigma_{eo} \bar{V}_e = n_0\, 5.0\times10^{-15} \sqrt{\frac{T_e}{m_e}}$$

5. ν_E (Energy confinement time rate) [***empirical law from "Alcator scaling"***]

$$\tau_E = \frac{0.03}{8.0\times10^{13}} n_e \frac{a^2}{27.0}$$

$$\nu_E = \frac{1}{\tau_E} \Rightarrow \nu_E = \frac{1}{\tau_E}\frac{I_p}{I_c} \quad (\text{if } I_p > I_c,\ \nu_E = 0.0)$$

Power density calculations [W/cm^3]

1. P_{ECH} (ECH RF power absorbed by electron) [13]

$$P_{ECH} = P_0\left[1 - f_O e^{-\eta_O} - f_X e^{-\eta_X}\right]$$

Where η_O and η_X are dimensionless optical depths and f_O and f_X are the fractional powers for the ordinary and extraordinary modes, respectively.

$$\eta_o = \frac{\pi^2 R}{\lambda}\frac{T_e}{m}\frac{n_e}{n_c}\sqrt{1-\alpha}\left[1 + n_{\|}^{\,2}(0.5-\alpha)\right]^{-1}$$

$$\eta_X = \frac{\pi^2 R}{\lambda}\frac{T_e}{m} n_{\|}^{\,2}(2-\alpha)^{3/2}(1+\alpha)^2\alpha^{-1}$$

Where $\alpha = n_c / n_c$ and $n_c = m\varepsilon_0\omega^2 / e^2$ is the critical density and $n_{\|}$ is the refractive parallel index.
If 1- $\alpha \le 0$, o-mode is cutoff (that is $\eta_O = 0.0$) and if 2- $\alpha \le 0$, x-mode is cutoff (that is $\eta_X = 0.0$).

2. P_{OH} (Ohmic heating power)

$$P_{OH} = I_p^2 R_p$$

Where I_p is the plasma current and R_p is the plasma resistance given before.

3. P_{RAD} (The radiation power loss from the ionizing process, e-i pair production loss) [7]

$$P_{RAD} = E_i n_e \nu_{ion}$$

Where $E_i = (W_{ion} + W_{rad}) = 4.8 \times 10^{-18}$ J = 30 eV for Hydrogen atom.

4. P_{EQU} (Electron-ion equipartition power loss) [7]

Power transferred from the electrons to ions (Hydrogen ions and impurity ions) through the collisions.

$$P_{EQU} = 7.75 \times 10^{-34} \left(T_e[eV] - T_i[eV]\right) \frac{n_e \ln \Lambda}{T_e^{3/2}[eV]} \left(\frac{n_H}{2} + \sum_I \frac{n_I Z_I^{\,2}}{A_I} \right) [W]$$

Where n_H is the Hydrogen ion density, n_I is the impurity ion density and the relation between electron density and ion densities is given by the charge conservation,

$$n_H = n_e - \sum_I Z_I n_I$$

The impurity ion density is assumed to be produced with **variable influx rate, $n_I = f_I n_e$**, where f_I is the fractional value of electron density, for the **constant n_I / n_H**. A_I is the impurity atomic mass number and the Z_I is the impurity atomic number. The summation is over impurity species, such as carbon and oxygen.

After this, the f_I is ***fci*** for the Carbon impurity and f_I is ***foi*** for Oxygen impurity and is set to 2 times of ***fci***.

5. P_{BREM} (Bremsstrahlung power loss) [7]

The power loss from interaction with both hydrogen ions and impurity ions.

$$P_{BREM} = 1.53 \times 10^{-38} n_e^{\,2} T_e^{\,1/2} [eV] Z_{eff} \quad [W]$$

$$\text{where, } Z_{eff} = \frac{n_H + \sum_I n_I Z_I^2}{n_e}$$

6. P_{CX} (Charge-exchange power loss) [7]

$$P_{CX} = \frac{3}{2} e n_H n_0 \left(T_i[eV] - T_0[eV]\right) S_{CX} \quad [W]$$

Where S_{CX} is the charge exchange rate coefficient and given by, $S_{CX} = 1.066 \times 10^{-8} \left(T_i[eV]\right)^{0.327}$

7. P_{CRAD} **and** P_{ORAD} (Carbon and oxygen impurity radiation) [14]

$$P = n_e n_I \times 10^f \times 10^6 \quad [W/cm^3]$$

Where,

f = -33.93 + 4.888 Q – 2.432 Q^2 + 0.3697 Q^3 for Carbon impurity,

f = -34.06 + 4.194 Q – 1.827 Q^2 + 0.2467 Q^3 for Oxygen impurity and Q = log10(T_e).

This form is given by fitting the data in the ref. [14].

Temporal behaviors with the inductance form of *Maroli and Petrillo*

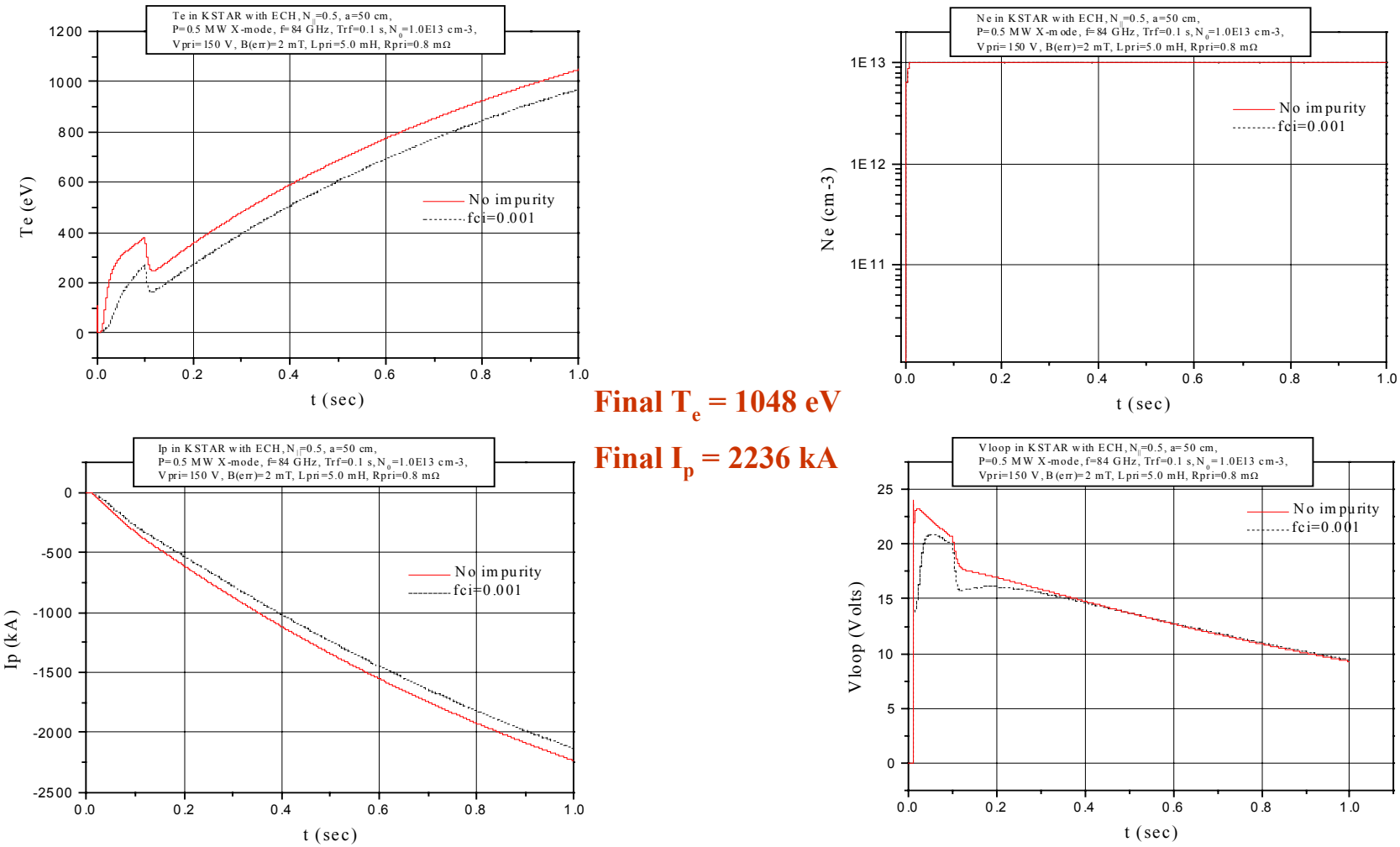

Figure 1. Temporal behavior for the first 1.0 s of the electron temperature, electron density, plasma current, and loop voltage for the present model. A microwave power level of 0.5 MW at 84 GHz is applied to a tokamak with R = 1.8 m, a = 50 cm, and B = 3 T. The error field is 2 mT.

Temporal behaviors with the inductance form of *B. Lloyd et al.*

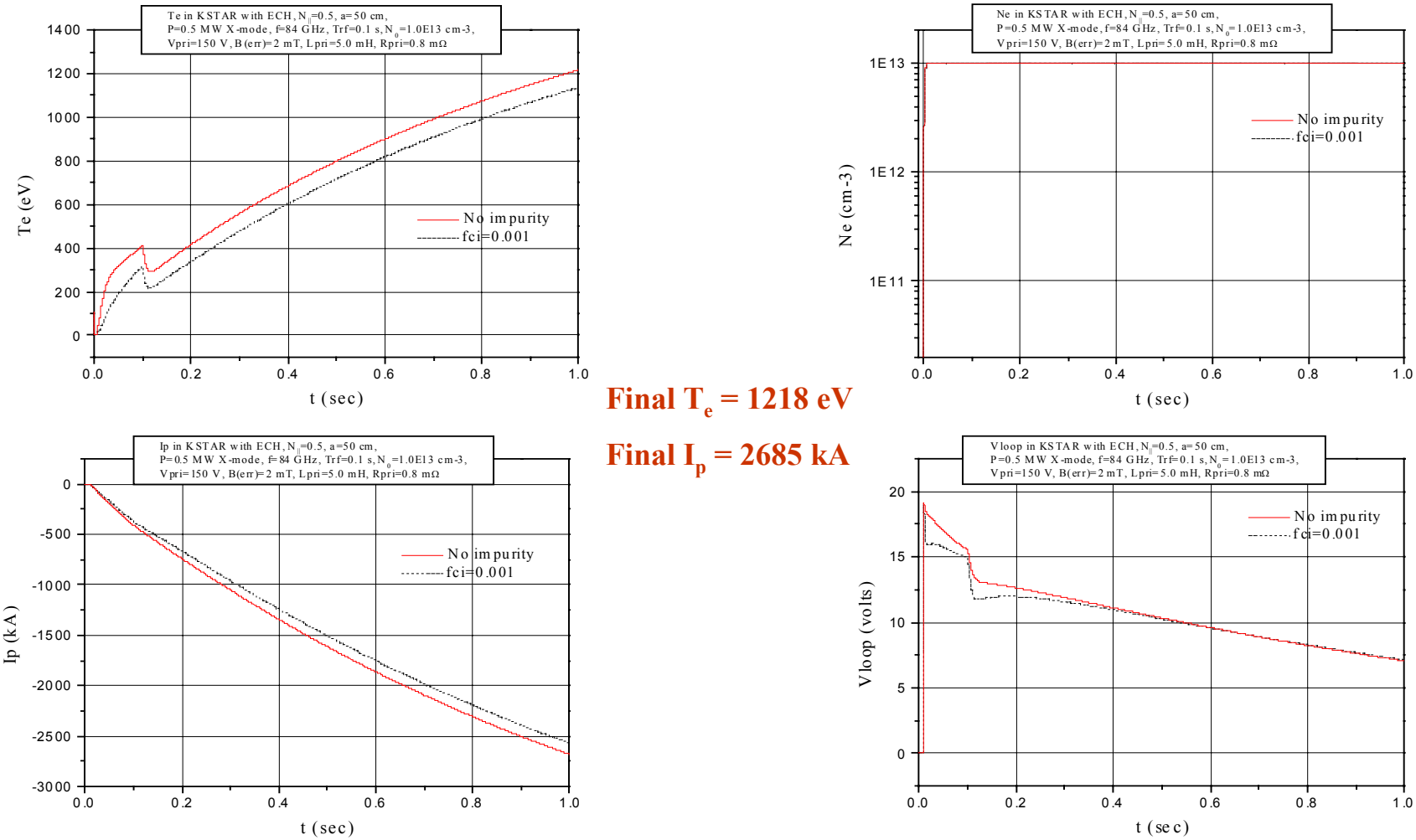

Final T_e = 1218 eV

Final I_p = 2685 kA

Figure 2. Temporal behavior for the first 1.0 s of the electron temperature, electron density, plasma current, and loop voltage for the present model with a different formula of plasma self inductance. A microwave power level of 0.5 MW at 84 GHz is applied to a tokamak with R = 1.8 m, a = 50 cm, and B = 3 T. The error field is 2 mT.

Carbon and Oxygen impurity effects

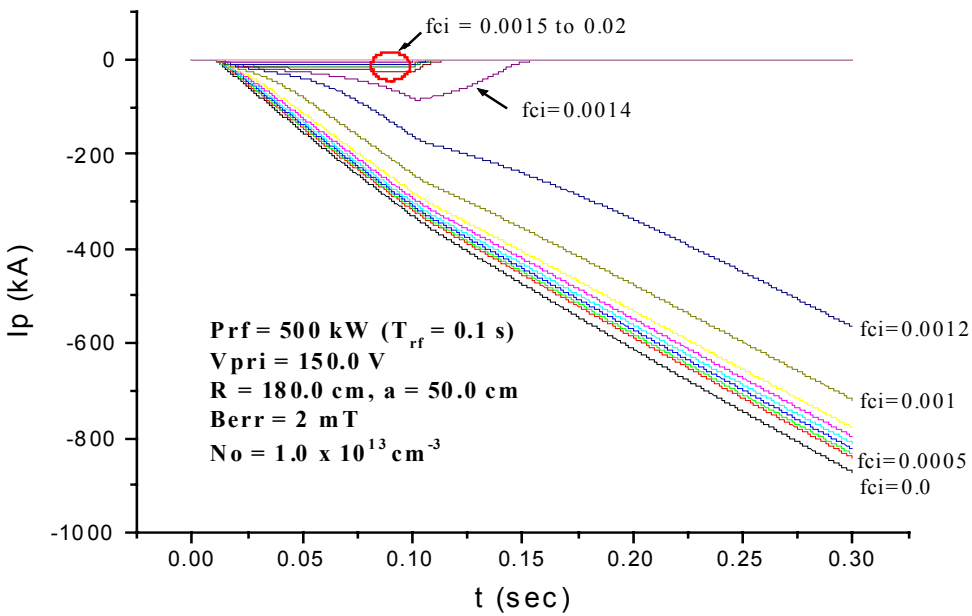

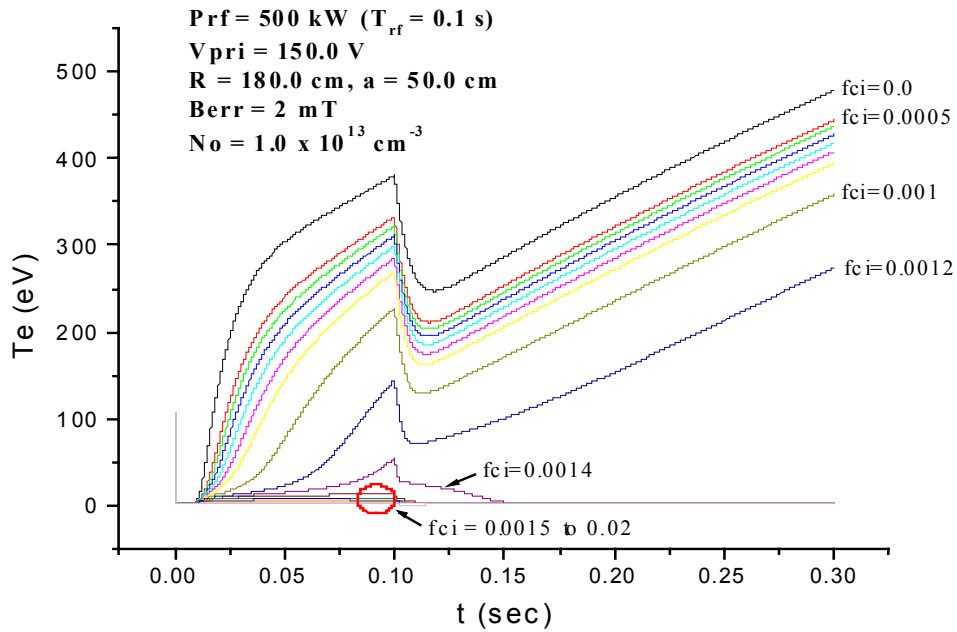

Figure 3. The temporal behaviors of electron temperature and plasma current as Carbon and Oxygen impurity fraction of electron density grow. The electron temperature and plasma current decay after the time of 0.1 s in case of fci = 0.0014 as seen in the above graphs.

Initial neutral density & RF power scan

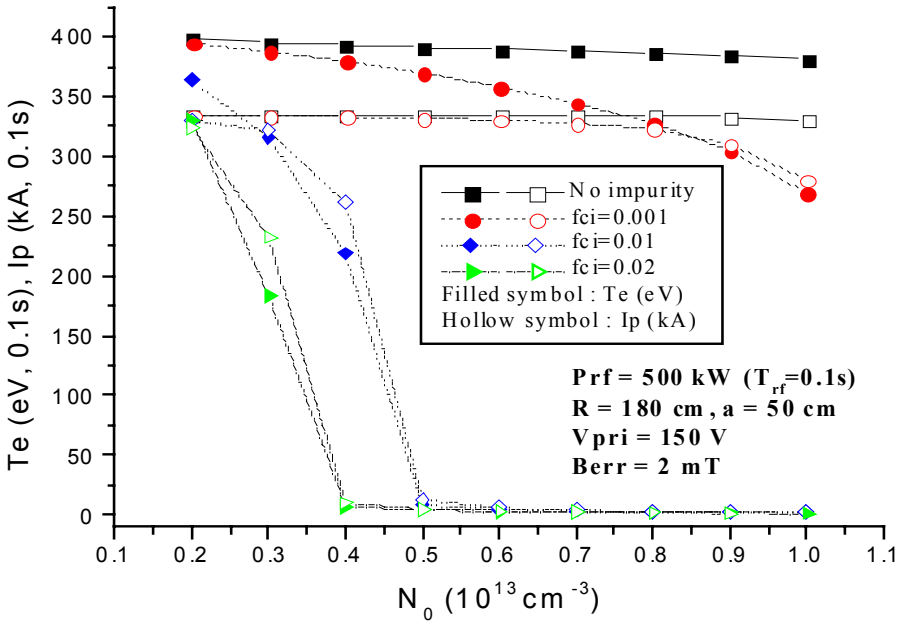

Figure 4. Electron temperature T_e(0.1 s) and plasma current I_p(0.1 s) as a function of the initial neutral density $\mathbf{N_e}$. While both T_e and I_p drop slightly with an increase in $\mathbf{n_0}$ in case of no impurity, they show very little variation with the initial neutral density. However, there is dramatic decay of T_e and I_p with impurities of **fci ≥ 0.01** and there is high variation in either Te or Ip with impurities of **fci = 0.001**.

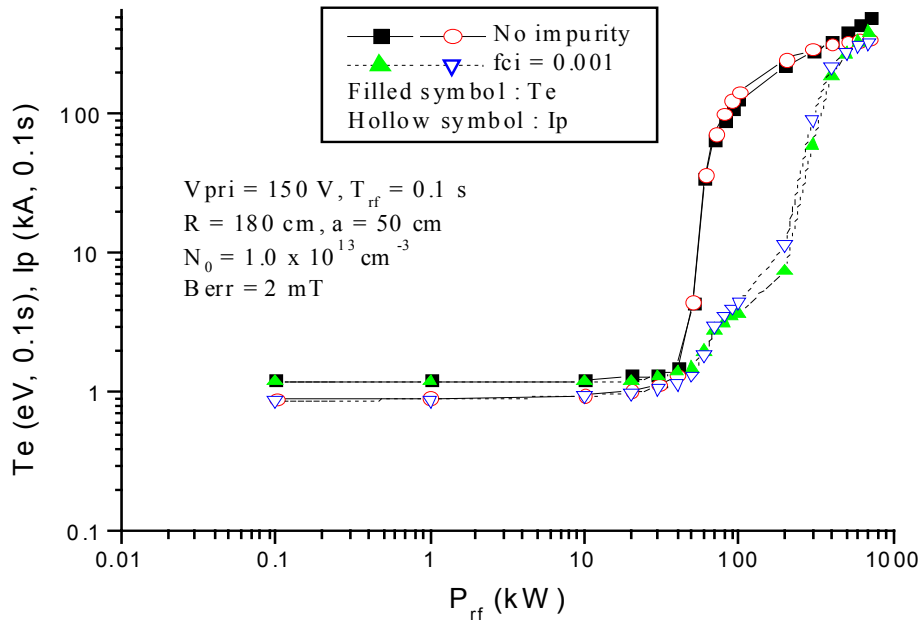

Figure 5. Electron temperature T_e(0.1 s) and plasma current I_p(0.1 s) vs. the applied RF power $\mathbf{P_{rf}}$. At a critical value of $\mathbf{P_{rf}}$ near **50 – 70 kW**, the temperature and current suddenly increase in both cases of no impurity and with impurity except the smaller increasing rate in case of with impurity.

Critical power, P_{rf_crit} & first zero ν_{err} time, t_{err}

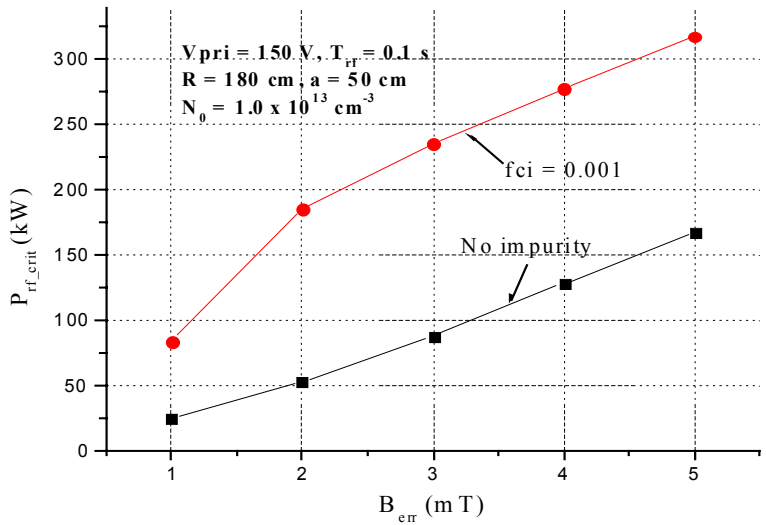

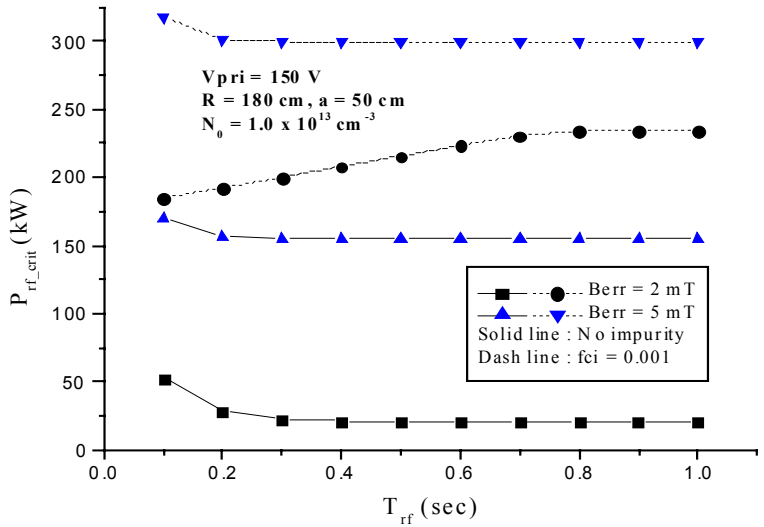

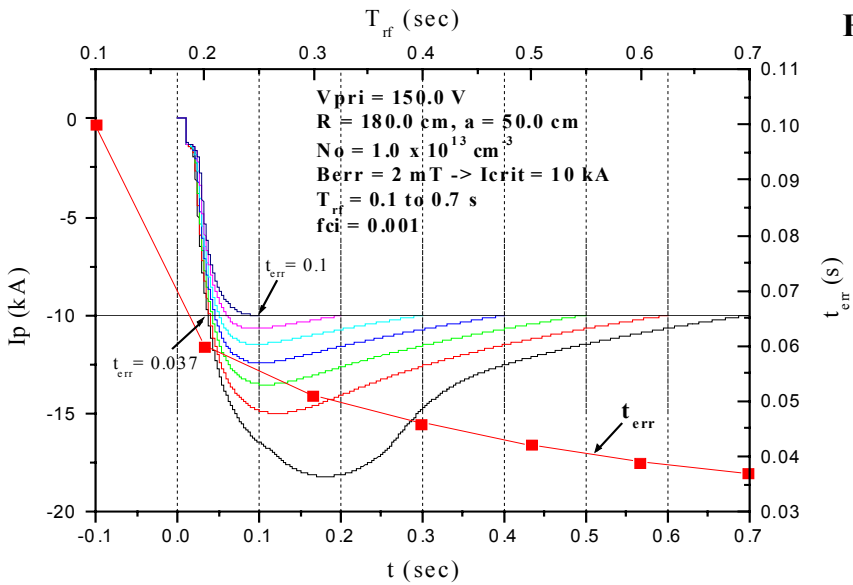

Figure 6 (up). The critical RF power, $\mathbf{P_{rf\_crit}}$ vs. error field (left) and T_{rf} (right). The value of P_{rf} at the value of I_p where the error field loss goes to zero is defined as $\mathbf{P_{rf\_crit}}$. The power required at B_{err} = 5 mT is less than the 500 kW available from the gyrotron with no impurity. With impurity (fci = 0.001), the power required at Berr = 5 mT is much higher than the power required in case of no impurity. In case of P_{rf_crit} vs. T_{rf}, P_{rf_crit} decreases to 21 kW for long pulses for the B_{err} = 2 mT and P_{rf_crit} decreases 155 kW for the B_{err} = 5 mT with no impurity. When impurities exist, P_{rf_crit} decrease to 300 kW for the B_{err} = 5 mT.

Figure 7 (left). The plasma current $\mathbf{I_p(t)}$ with given $\mathbf{P_{rf\_crit}}$ of pulse duration of T_{rf} and first zero loss time $\mathbf{t_{err}}$ for the B_{err} = 2 mT when impurities exist. This plot shows the first zero error loss time $\mathbf{t_{err}}$ is less than T_{rf} from the current change of time. This means that the error field loss goes to zero at time much less than T_{rf} with given $\mathbf{P_{rf\_crit}}$ which is defined as the value of RF power at the value of I_p where error field loss goes to zero at $\mathbf{t = T_{rf}}$.

Primary voltage scan & error field scan

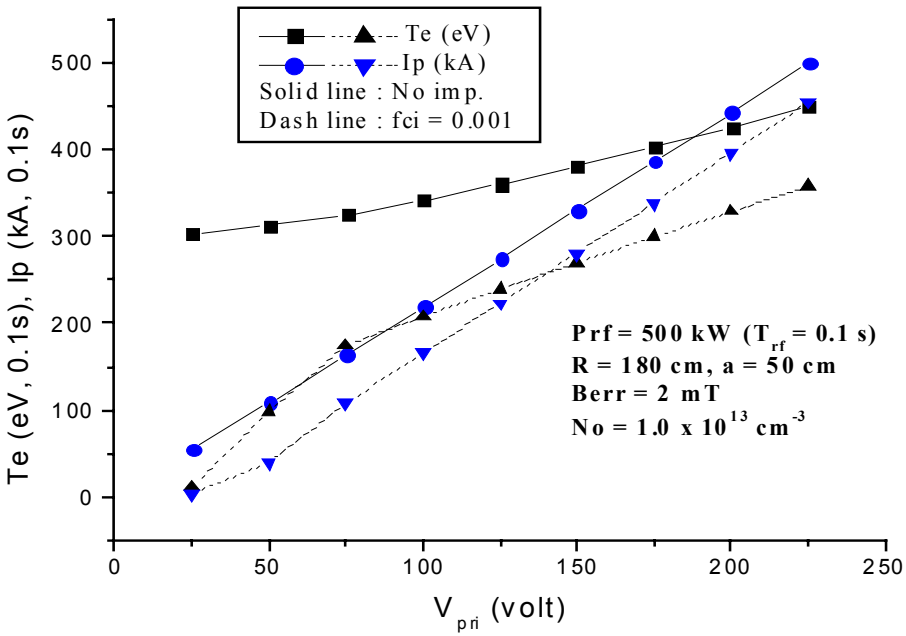

Figure 8. Values of T_e and I_p at t = 0.1 s as a function of primary voltage $\mathbf{V_{pri}}$. The plasma current increases linearly with the primary voltage and the electron temperature also increases slowly with the primary voltage.

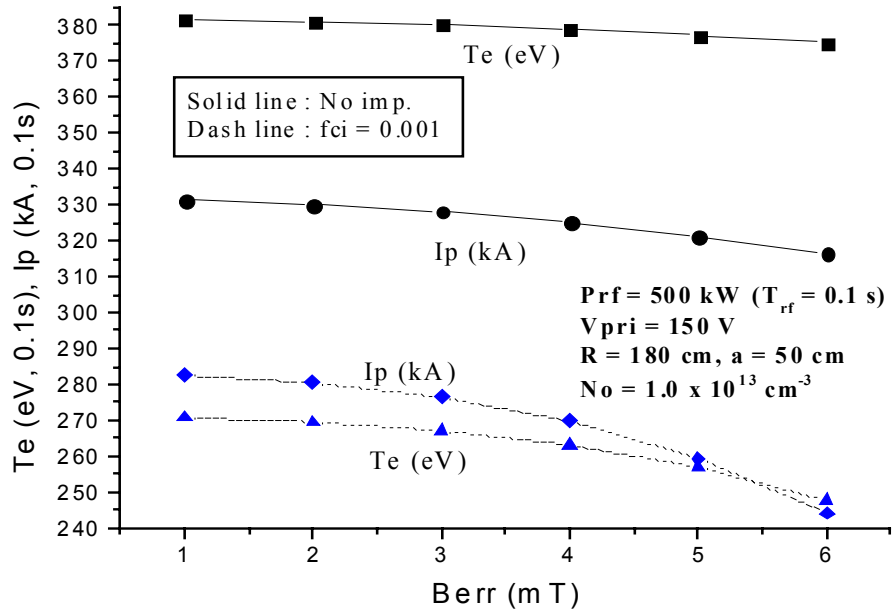

Figure 9. T_e (eV) and I_p (kA) at t = 0.1 s as a function of error field $\mathbf{B_{err}}$ **(mT)**. The plasma current and electron temperature decrease slowly as the error field increases with no impurity, but when impurities exist, the current and temperature decrease fast.

Threshold primary voltage

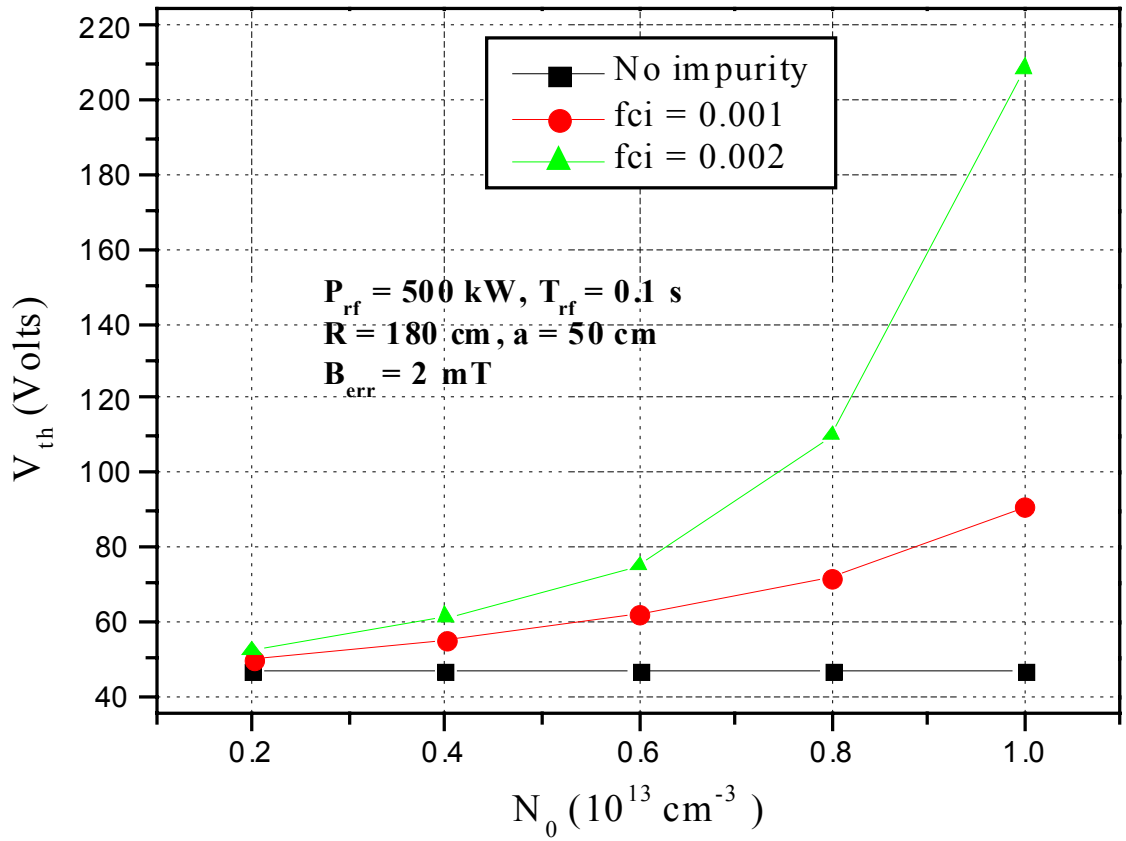

Figure 10. The threshold voltage vs. neutral density. The threshold voltage is defined as the primary voltage below which the plasma current decay after the RF ends. The RF duration is 0.1 s. The threshold voltage has no dependence of neutral density when there exist no impurities. When there exist impurities, the threshold voltage increases as the neutral density increases and its growth rate increases as the impurity fraction increases.

Future studies

- **Plasma expanding in minor radius with time [9]:**

$$a(t) = a_0(t=0) + \left[0.4 \frac{q_c(t) I_p(t) R}{(1+\sigma^2) B_T} \right]^{1/2}$$

$$\text{where, } q_c(t) = 6.67 \times 10^6 \frac{T_e^{1/2}}{R(\nu_{dr} + \nu_{err})}$$

where σ is vertical elongation (σ = 2.0 for KSTAR).

- **The effects of other impurities such as Iron and Molybdenum;**

The radiation power from these impurities are also given by the fitting in ref. [14].

- **The seven pairs of independently controlled poloidal field coils;**

Circuit equations need to be changed with independently controlled coil current scenarios.

References

[1] Y-K, M. Peng et al., Nuclear Fusion, **18**, 1489, (1978)

[2] A. G. Kulchar et al., Phys. Fluids, **27**, 1869, (1984)

[3] V. V. Alikaev et al., Controlled Fusion and Plasma Heating, (Proc. 17th Eur. Conf. Amsterdam, 1990), Vol. **14B**, Part III, EPS, 1084, (1990)

[4] B. Lloyd et al., Nuclear Fusion, **31**, 2031, (1991)

[5] I. Fidone and G. Granata, Nuclear Fusion, **34**, 743, (1994)

[6] C. Maroli and V. Petrillo, Il Nuovo Cimento, Vol. **10**, No. 6, 677, (1988)

[7] B. Lloyd et al., Plasma Phys. Control. Fusion, **38**, 1627, (1996)

[8] KSTAR Physics Validation Review Documents, Korea Basic Science Institute, 22-25 June 1997 (unpublished)

[9] NRL Plasma Formulary, 1998 (revised)

[10] R. L. Freeman and E. M. Jones, Culham Laboratory Report **137**, May 1974

[11] Francis F. Chen, "Introduction to Plasma Physics and Controlled Fusion", 2nd Edit., Vol. 1, pp **43**, (1984)

[12] Michael A. Lieberman and Allan J. Lichtenberg, "Principles of Plasma Discharges and Materials Processing", pp **142-143**, (1994)

[13] Owen C. Eldridge et al., Oak Ridge National Laboratory Technical Report 6052, (1977)

[14] P. G. Carolan and V. A. Piotrowicz, Plasma Phys. Vol. **25**, No. 10, 1065, (1983)